TISSUE ENGINEERING: Part A
Volume 19, Numbers 7 and 8, 2013

DOI: 10.1089/ten.tea.2012.0088

Regenerative Potential of Decellularized Porcine *Nucleus Pulposus* Hydrogel Scaffolds: Stem Cell Differentiation, Matrix Remodeling, and Biocompatibility Studies

Jeremy J. Mercuri, PhD,[1] Sourav Patnaik, MS,[2] Grace Dion, BS,[1] Sanjitpal S. Gill, MD,[3] Jun Liao, PhD,[2] and Dan T. Simionescu, PhD[1]

Nucleus pulposus (NP) tissue regeneration has been proposed as an early stage interventional therapy to combat intervertebral disc degeneration. We have previously reported on the development and characterization of a novel biomimetic acellular porcine NP (APNP) hydrogel. Herein, we aimed to evaluate this material for use as a suitable scaffold for NP tissue regeneration. Human-adipose-derived stem cells (hADSCs) were cultured for 14 days on APNP hydrogels in chemically defined differentiation media and were analyzed for an NP-cell-like mRNA expression profile, evidence of hydrogel remodeling including hydrogel contraction measurements, extracellular matrix production, and compressive dynamic mechanical properties. The innate capacity of the hydrogel itself to induce stem cell differentiation was also examined via culture in media lacking soluble differentiation factors. Additionally, the *in vivo* biocompatibility of non-crosslinked and ethyldimethylaminopropyl carbodiimide/N-hydroxysuccinimide and pentagalloyl glucose crosslinked hydrogels was evaluated in a rat subdermal model. Results indicated that hADSCs expressed putative NP-cell-positive gene transcript markers when cultured on APNP hydrogels. Additionally, glycosaminoglycan and collagen content of hADSC-seeded hydrogels was significantly greater than nonseeded controls and cell-seeded hydrogels exhibited evidence of contraction and tissue inhibitors of metalloproteinase-1 production. The dynamic mechanical properties of the hADSC-seeded hydrogels increased with time in culture in comparison to noncell-seeded controls and approached values reported for native NP tissue. Immunohistochemical analysis of explants illustrated the presence of mononuclear cells, including macrophages and fibroblasts, as well as blood vessel infiltration and collagen deposition within the implant interstices after 4 weeks of implantation. Taken together, these results suggest that APNP hydrogels, in concert with autologous ADSCs, may serve as a suitable scaffold for NP tissue regeneration.

Introduction

Progressive and symptomatic intervertebral disc (IVD) degeneration is a multifactor process that places significant social and economic burden on society. Nearly 5.7 million Americans are diagnosed with IVD disorders annually.[1] Conservative estimates indicate that spine-related maladies, including IVD degeneration, ranked 12th among most frequent diagnosis accounting for 635,915 hospitalizations in 2006 resulting in an aggregate cost of approximately $6.7 billion in the United States alone.[2] It has been recognized that the degenerative process first manifests within the nucleus pulposus (NP) region of the IVD.[3,4] This centrally located hydrogel core of the IVD, composed predominantly of aggrecan and type II collagen, undergoes aberrant changes in its cellular and biochemical components resulting in its eventual desiccation and compromised mechanical function.[5,6]

Accordingly, numerous strategies targeting the replacement of the NP are being developed as early stage interventional therapies to slow or halt the progression of degeneration. One such strategy, tissue engineering, has shown some efficacy toward regenerating NP tissue via the use of autologous cells in conjunction with various scaffolds that attempt to mimic the physico-chemical characteristics of the native NP extracellular matrix (ECM).[7–10] Taking one step beyond the basic principle

[1]Department of Bioengineering, Clemson University, Clemson, South Carolina.
[2]Department of Agricultural & Biological Engineering, Mississippi State University, Starkville, Mississippi.
[3]Department of Orthopaedic Surgery, The Village at Pelham, Greer, South Carolina.

that a scaffold material should mimic the prominent characteristics of the native tissue microarchitecture, it is important that the scaffold supports an appropriate, tissue-specific cell phenotype. This is especially true when utilizing stem cells as an alternative cell source for tissue engineering applications. Differentiation of stem cells into an appropriate phenotype, which can be influenced in part by scaffold mechanical properties and composition, is important for regenerating a specific tissue of interest. Moreover, cells in contact with the scaffold material should maintain the ability to remodel the initial support structure, decomposing it and subsequently replacing it with a tissue-specific ECM. In considering these points in the specific context of NP tissue regeneration, an appropriate NP-cell-like phenotype should be maintained by the chosen scaffold material. This would be indicated in part by cellular mRNA expression of key NP ECM components and cellular transcription factors. Moreover, round cell morphology, production of sulfated glycosaminoglycan (GAG), and evidence of cell-mediated remodeling should all be considered requirements sought in a scaffold used for NP tissue regeneration. Additionally, considering the long-term objective of delivering a scaffold into the body of a patient, the material must exhibit evidence of *in vivo* biocompatibility. A severe sustained inflammatory or immune response should not be elicited by the scaffold and evidence of favorable host remodeling should be observed.

We have previously reported on the development and characterization of a novel biomimetic hydrogel derived from decellularized porcine NP tissue.[11] This material, which will be referred to herein as the "APNP hydrogel," has been shown to exhibit biochemical and mechanical characteristics comparable to that of human NP and allows for repopulation and maintenance of viability of a human stem cell source.[11] The present study was aimed at further evaluating our novel APNP hydrogel material for use as a suitable scaffold for NP tissue regeneration. This included investigating the ability of our hydrogel to support human-adipose-derived stem cell (hADSC) differentiation toward an NP-cell-like phenotype, its ability to be remodeled by the hADSCs, and examination of APNP hydrogel *in vivo* biocompatibility.

Materials and Methods

APNP hydrogel preparation

APNP hydrogels were prepared as previously reported.[11] Briefly, samples were harvested from the spines of juvenile pigs in a decellularization solution of 50 mM Tris (Hydroxymethyl)-aminomethane buffer (pH 7.5) containing 1% (w/v) deoxycholic acid, 0.6% Triton X-100 (v/v), 0.1% (w/v) ethylenediamine tetraacetic acid, and 0.02% (w/v) sodium azide. Samples were subsequently decellularized in this solution for a total of 72 h with fresh changes of solution and 10-min periods of ultrasonication occurring every 24 h followed by treatment with a mixture of nucleases (720 mU/mL deoxyribonuclease and 720 mU/mL ribonuclease in a phosphate-buffered saline containing 5 mM magnesium chloride [pH 7.5]) for 48 h prior to sterilization with 0.1% peracetic acid for 4 h.

For *in vivo* biocompatibility studies, APNP hydrogels were randomized into three study groups: (1) nonchemically crosslinked (denoted as "nonfixed," $n=10$), (2) chemically crosslinked with 30 mM ethyldimethylaminopropyl carbodiimide and 6 mM N-hydroxysuccinimide for 24 h (denoted as "EDC/NHS fixed," $n=10$), or (3) chemically crosslinked with an EDC/NHS (described just now) followed by 24 h in 0.15% pentagalloyl glucose (PGG; a generous gift from N.V. Ajinomoto OmniChem S.A., Wetteren, Belgium) (denoted as "EDC/NHS + PGG fixed," $n=10$). Following crosslinking, all hydrogels were sterilized in 0.1% peracetic acid, rinsed in sterile water, lyophilized, and then stored in sterile 2 mL microfuge tubes prior to implantation.

ADSC culture and differentiation on APNP hydrogels

hADSCs (Passage 2–3; Invitrogen) were seeded onto sterile APNP hydrogels at a density of 2,000 cells/mm^2 and were cultured for 14 days at 5% carbon dioxide and 37°C in either differentiation media or Dulbecco's modified Eagle's medium (DMEM) in 24-well plates. Differentiation media were composed of DMEM with the addition of 1% fetal bovine serum (FBS), 1% antibiotic/antimycotic (Ab/Am), 5 μg/mL insulin, 5 μg/mL transferrin, 5 ng/mL sodium selenite, 10 ng/mL transforming growth factor-β (TGF-β), and 50 nM ascorbate-2-phosphate. For comparison, hADSC-seeded APNP hydrogels cultured in regular DMEM containing 10% FBS and 1% Ab/Am were also evaluated. Nonseeded hADSC hydrogels cultured in both media types served as controls for biochemical assays. Monolayer cultures of hADSCs in stromal growth media (Invitrogen)—used to maintain stem cells in an undifferentiated state—were used for normalization of gene analysis data. RNA isolated from fresh juvenile porcine NP and articular cartilage tissue was also used for additional comparison. Briefly, porcine NP samples from six cervical discs were harvested in DMEM containing 10% FBS and 1% Ab/Am. RNA from these samples was isolated within 2 h of harvest. Cartilage samples (5-mm-diameter × 1.5-mm-thick biopsies) were obtained from the medial condyles of six different pigs and were placed into RNAlater solution until RNA isolation. Stem-cell-seeded hydrogel samples were harvested at 7- and 14-day time points for analysis. Samples used for gene expression ($n=3$ per study group) and biochemical evaluation ($n=6$ per study group) were snap frozen and stored at −80°C until time of analysis. Samples for biomechanical analysis ($n=5$ per study group) were maintained in media immediately prior to testing. Samples used for histological analysis were stored in 10% neutral buffered formalin prior to standard histological processing.

Reverse transcription–polymerase chain reaction gene analysis

Total RNA from hADSC-seeded APNP hydrogel constructs, monolayer controls, and porcine NP and cartilage tissue was isolated using Trizol reagent (Invitrogen) according to the manufacturer's instructions. RNA integrity and quantification was assessed using an Agilent 2100 Bioanalyzer with RNA 6000 Nano microfluidics chips according to the manufacturer's instructions. A total of < 1 μg of RNA was reverse transcribed using an Ambion Retroscript kit containing oligo dTs, reaction buffer, dNTPs, RNase inhibitors, and reverse transcriptase. Resulting cDNA was amplified using a Rotogene 3000 thermocycler. Reaction products were detected using human and porcine primer sequences (Table 1) in conjunction with a QuantiTect SYBR green polymerase chain reaction (PCR) kit. The gene

Table 1. Human and Porcine Primer Sequences Used for Reverse Transcriptase–Polymerase Chain Reaction Experiments

Gene name	*Species*	*Gene symbol*	*Forward primer sequences*	*Reverse primer sequences*
Aggrecan	Human	*ACAN*	CAA CTA CCC GGC CAT CC	GAT GGC TCT GTA ATG GAA CAC
Sex determining region y–box 9	Human	*SOX-9*	GAC TTC CGC GAC GTG GAC	CAG TAC CTG CCG CCC AAC
Type II collagen	Human	*COL2A1*	GGC AAT AGC AGG TTC ACG TAC A	CGA TAA CAG TCT TGC CCC ACT T
Type III collagen	Human	*COL3A1*	AGA AGG CCC TGA AGC TGA TG	TGT TTC GTG CAA CCA TCC TC
Tissue inhibitor of metalloproteinase-1	Human	*TIMP-1*	CTG TTG GCT GTG AGG AAT GC	CAA GGT GAC GGG ACT GGA AG
Paired box 1	Human	*PAX-1*	TGG CCC TCG GCT CAT TC	GCC CCT GTT TGC TCC ATA AA
Integrin binding sialoprotein	Human	*IBSP*	CCA GAG GAA GCA ATC ACC AAA	GCA CAG GCC ATT CCC AAA
18s	Human	*18S*	GTA ACC CGT TGA ACC CCA TT	GTA ACC CGT TGA ACC CCA TT
Aggrecan	Porcine	*ACAN*	CGC TGG TCA GAT GGA CAC TC	TCT CGT GCC AGA TCA TCA CC
Sex determining region y–box 9	Porcine	*SOX-9*	CAG CGA ACG CAC ATC AAG AC	GTA GTG CGG GAG GTT GAA GG
Type II collagen	Porcine	*COL2A1*	CAA AGA TGG CGA GAC AGG TG	AAG TCC CTG GAA GCC AGA TG
Type III collagen	Porcine	*COL3A1*	TGG CAT CAA AGG ACA TCG AG	ACT CGG TCC AAC AGG TCC TC
Tissue inhibitor of metalloproteinase-1	Porcine	*TIMP-1*	CTA TGC TGC TGG CTG TGA GG	CTG GAA GCC CTT GTC AGA GC
Paired box 1	Porcine	*PAX-1*	GCC ATG ACC TTC AAG CAT CC	GGA TGG GCA GTC CGT GTA AG
Integrin binding sialoprotein	Porcine	*IBSP*	CCT CCA GCT TCC CAA GAA GG	GTG CCT TGC TCG TTG TCA TC
Glyceraldehyde-3-phosphate dehydrogenase	Porcine	*GAPDH*	GGA CCA GGT TGT GTC CTG TG	CCA CCA CCC TGT TGC TGT AG

expression ratio for each marker was quantified mathematically by the $2^{-\Delta\Delta Ct}$ method using 18S or *GAPDH* as the housekeeping gene and by comparing target genes relative to undifferentiated hADSC controls. It should be noted that undifferentiated hADSCs did not express paired box 1 (*PAX-1*) and thus expression data for this gene were normalized to the day-7 DMEM group.

DNA, GAG, hydroxyproline, and water content analysis

Snap-frozen hADSC-seeded APNP hydrogels and nonseeded controls were lyophilized, dry weights were recorded, and samples were digested using 125 μg/mL papain in a 100 mM dibasic phosphate buffer solution (pH 7.5). Each individual sample was analyzed for DNA, sulfated GAG, and hydroxyproline (Hyp) content. Double-stranded DNA content was determined via a Quant-iT™ PicoGreen® assay kit (Invitrogen) in accordance with manufacturer's protocol. Total double-stranded DNA content in each sample was determined from a standard curve developed from serial dilutions of DNA stock provided.

Total sulfated GAG content was quantified using the dimethylmethylene blue assay as described by Farndale and colleagues.[12] GAG content was determined via a standard curve developed from serial dilutions of known concentrations of chondroitin sulfate sodium salt. Values were normalized to sample dry weights and DNA content.

Hyp content was quantified according to methods adapted from Blumenkrantz and Asboe-Hansen.[13] Hyp content was determined using a standard curve of known concentrations of Hyp. Data were normalized to sample dry weights and DNA content.

Water content of hADSC-seeded and nonseeded hydrogels was determined gravimetrically by measuring sample wet weights and their corresponding dry weights following lyophilization. Percent water content was calculated by dividing the difference between the wet and dry weights by the dry weight.

APNP hydrogel contraction measurements

Contraction of representative APNP hydrogels ($n=6$ per study group) was tracked daily for a total of 14 days via photo capture using a digital camera. Using NIH Image-J software, captured color images were converted to scaled 8-bit gray-scale files and thresholded using binary processing. The surface area of each hydrogel was then measured using the "analyze particles" processing option. The average surface area of the APNP hydrogels ($n=6$ per study group per time point) was plotted with respect to time in culture.

Cell viability and histological analysis

Assessment of hADSC viability on APNP hydrogels ($n=4$ per time point per study group) was assessed at 2, 7, and 14 days using a LIVE/DEAD® staining kit (Molecular Probes) according to manufacturer's instructions. Controls for LIVE/DEAD assay were prepared by the addition of 70% ethanol for 30 min to cell-seeded hydrogels yielding 100% red staining indicative of cell death. LIVE/DEAD images were captured using an Olympus IX81 confocal microscope. Six representative 200× total magnification images for each time point in each culture condition were evaluated. The number of live cells within each image were counted and

expressed as a percentage of total cell number (% cell viability). Histological analysis was performed on formalin-fixed samples embedded in paraffin and sectioned at 5-μm thicknesses. Representative sections were stained with hematoxylin and eosin, Alcian blue with Brazilliant!® nuclear fast red counter-stain, and Movat's Pentachrome.

Matrix metalloproteinase/tissue inhibitors of metalloproteinase array analysis

The presence of matrix metalloproteinases (MMPs) and tissue inhibitors of metalloproteinases (TIMPs) within hADSC-seeded APNP hydrogels ($n=3$ per time point per study group) was evaluated using an antibody array (Raybiotech) according to manufacturer's instructions. Briefly, total protein was extracted using lysis buffer and quantified using the bicinchoninic assay (Pierce). Two hundred fifty micrograms of protein was incubated on the array membranes for 2 h prior to washing the membranes and incubation in biotin-conjugated primary antibodies. The presence of MMPs/TIMPs was detected using chemiluminescence imaging and quantified using a Fluorchem SP imaging system with charge-coupled device camera (Alpha Innotech). Values are expressed as an average integrated density value normalized to noncell-seeded hydrogels.

Dynamic mechanical analysis

Complex modulus and phase angle measurements of hADSC-seeded APNP hydrogels cultured for 7 and 14 days in differentiation media or DMEM were evaluated and compared with nonseeded APNP hydrogel controls. The protocol for testing was modeled based on a previously published study on sheep NP.[14] Samples from each study group were subjected to unconfined compression using dynamic mechanical analyzer (DMA Q 800; TA Instruments). All samples used for testing had a thickness ranging from 1.5 to 1.55 mm. After the samples were mounted onto the DMA system, a small preload (0.5 g) was applied to produce a gauge length of ~1.5 mm. The oscillatory amplitude was set at 15 μm, which generated a dynamic strain level of 1%. Samples were kept moist while subjected to testing at ~23°C for ~2–4 min. During testing, the hood of the DMA remained closed and sample hydration status was maintained. Data were recorded over a range of frequencies (0.1, 1, 10, and 40 Hz).

In vivo *biocompatibility testing*

Male juvenile Sprague–Dawley rats ($n=20$) weighing between 35 and 40 g were utilized for the study. Animals were placed under general anesthesia by inhalation of isoflurane gas. One small (10 mm) incision was made transversely to the dorsal midline of each animal in which two subdermal pockets were made by blunt dissection. One sterile APNP hydrogel was placed into each pocket, yielding two implants per rat. Incisions were closed with surgical staples. Acellular hydrogel study groups included (1) nonfixed APNP hydrogels, (2) EDC/NHS-fixed APNP hydrogels, and (3) EDC/NHS + PGG-fixed APNP hydrogels as described earlier. Four rats were randomly assigned to each study group, each receiving two implants. Additionally, two rats were used as negative controls according to ISO-10993 with each receiving two 2 mm × 2 mm implants composed of high-density polyethylene (HDPE). Following 4 weeks of implantation, rats were humanely euthanized via carbon dioxide inhalation. Implants and any associated capsule were explanted and prepared for histological analysis via submersion in 10% neutral buffered formalin. All animals received humane care in compliance with protocols approved by Clemson University Animal Research Committee and the NIH (Publication No. 86–23, Rev. 1996).

Explants were evaluated histologically and immunohistochemically for the presence of host cell phenotypes within and around the implanted hydrogels. Briefly, 5-μm sections were deparaffinized and rehydrated to water with graded ethanol. Gomori's one-step trichrome stain was used to indicate the presence of collagen within the explant and surrounding fibrous capsule; capsular thickness was measured with Zeiss AxioVision analysis software. Immunohistochemistry was used to discriminate between infiltrating host cell types. Heat-mediated antigen retrieval was performed in a microwave oven using 10 mM citric acid (pH 6.0) for 20 min at 90°C. Slides were permeabilized in 0.025% Triton X-100, nonspecific binding was blocked with normal serum, and endogenous peroxidases were blocked with 0.3% hydrogen peroxide in 0.3% normal serum. Primary antibodies that were used included mouse anti-rat anti-CD68 (macrophages: 2.5 μg/mL; Millipore), vimentin (fibroblasts: 2.5 μg/mL; Sigma), CD8 (T-cells: 20 μg/mL; GeneTex), and prolyl 4-hydroxylase (10 μg/mL; Millipore). Negative controls did not receive primary antibody. Rat-adsorbed anti-mouse IgG secondary antibody was utilized along with a diaminobenzidine tetrahydrochloride peroxidases substrate kit (Vector Laboratories) in order to visualize the specific staining. Sections were subsequently counterstained with a 50:50 mixture of hematoxylin in distilled water. Histological sections taken from rat spleen were used as positive controls for both macrophages and T-lymphocytes, and rat skin was used for vimentin-positive controls.

Statistics

Results are represented as a mean ± standard error of the mean. One-way analysis of variance using Fisher's least significant difference *post hoc* multiple comparison procedures and Student's *t*-test of unequal variance were used for statistical analysis when appropriate. Significance was defined in all cases as $p<0.05$.

Results

Reverse transcription–PCR gene analysis

Gene expression profiles of hADSCs seeded on the APNP hydrogels cultured in either DMEM or differentiation media were evaluated to determine whether an NP-cell-like gene expression profile could be achieved. By day 14, hADSCs seeded on APNP hydrogels cultured in both media conditions exhibited at least a twofold upregulation in all genes analyzed compared with undifferentiated stem cell controls (Fig. 1). Included in these genes were putative NP-cell-positive markers PAX-1, type III collagen, and TIMP-1. Type II collagen expression was significantly higher in the differentiation media group as compared with the DMEM group at both time points (ninefold vs. twofold increase,

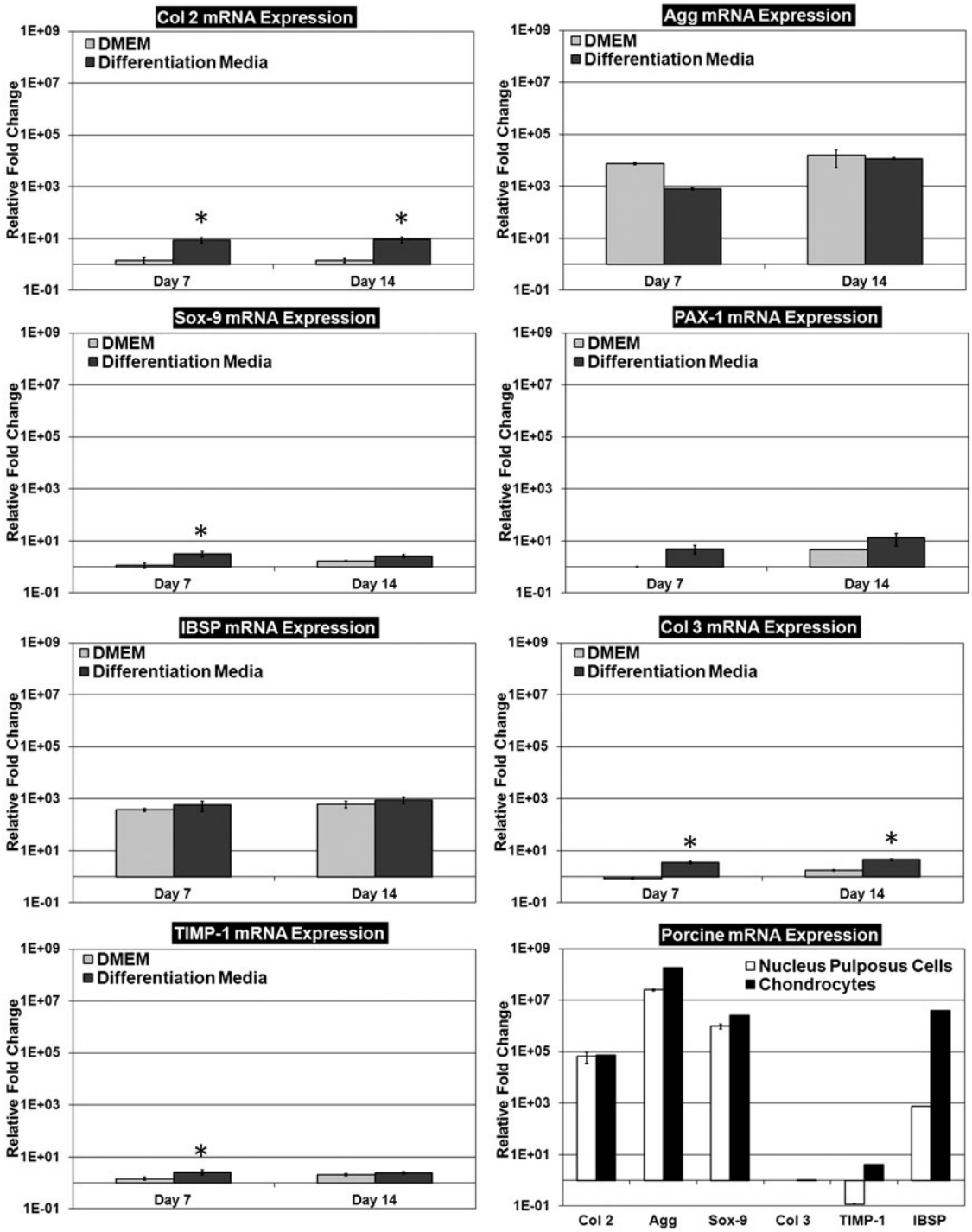

FIG. 1. Gene transcript profiles of human-adipose-derived stem cells seeded on acellular porcine nucleus pulposus (APNP) hydrogels cultured in Dulbecco's modified Eagle's medium (DMEM) or differentiation media. Analysis included examination of putative NP-cell-positive and chondrocyte-positive markers and the gene expression of porcine NP cells and articular chondrocytes. Progressive differentiation toward a mixed NP-cell- and chondrocyte-like phenotype was observed on APNP hydrogels. Note: Gene expression data are expressed as a relative fold change compared with undifferentiated stem cells maintained in stromal growth media in monolayer culture (negative control). The symbol * indicates a significant difference ($p < 0.05$) comparing between DMEM and differentiation media groups for each respective time point ($n = 3$ per study group per time point).

respectively). Additionally, *Sox-9*, type III collagen, and *TIMP-1* expression was found to be significantly greater in the differentiation media group compared with the DMEM group. *PAX-1* expression trended toward being greater in the differentiation media group (13-fold increase) compared with the DMEM group (approximately fivefold increase); however, no statistical difference was found. No differences were noted comparing between these two study groups for aggrecan or integrin binding sialoprotein (*IBSP*); both exhibited greater than a 10,000-fold increase in aggrecan and

500-fold increase in *IBSP* expression. Porcine NP cells and articular chondrocytes tended to have greater expression of the gene transcripts examined as compared with the hADSCs seeded on APNP hydrogels.

DNA, GAG, Hyp, and water content analysis

The DNA content found within hADSC-seeded APNP hydrogels was utilized in order to evaluate cell proliferation as well as for GAG and Hyp content data normalization. No significant change in DNA content was observed within the APNP hydrogels from day 7 to 14 regardless of culture media used (data not shown). GAG and Hyp content was evaluated in an attempt to elucidate hADSC-mediated production of these matrix molecules within the APNP hydrogels and thus they were used as indirect indicators of NP-like tissue formation. The GAG content found in hADSC-seeded hydrogels cultured in DMEM was significantly different ($p<0.05$) compared with nonseeded controls at day 7 (37.50 ± 4.84 vs. $18.3\pm2.05\,\mu g/mg$ dry weight, respectively); however, no statistical difference between these two groups was noted by day 14 (25.89 ± 3.37 vs. $20.6\pm2.66\,\mu g/mg$ dry weight) (Fig. 2A). The GAG content found within hADSC-seeded APNP hydrogels cultured in differentiation media (Fig. 2A) at day 7 and 14 (34.74 ± 3.58 and $46.28\pm3.78\,\mu g/mg$ dry weight, respectively) was significantly different ($p<0.05$) compared with nonseeded controls at each respective time point. GAG content measurements normalized to DNA indicated that the hydrogels cultured in differentiation media contained significantly more GAG compared with hydrogels cultured in DMEM at both the 7-day (differentiation media: $226.80\pm19.63\,\mu g/\mu g$ DNA vs. DMEM: $158.68\pm23.97\,\mu g/\mu g$ DNA) and 14-day time points (differentiation media: $173.24\pm7.29\,\mu g/\mu g$ DNA vs. DMEM: $104.51\pm25.52\,\mu g/\mu g$ DNA), respectively ($p<0.05$).

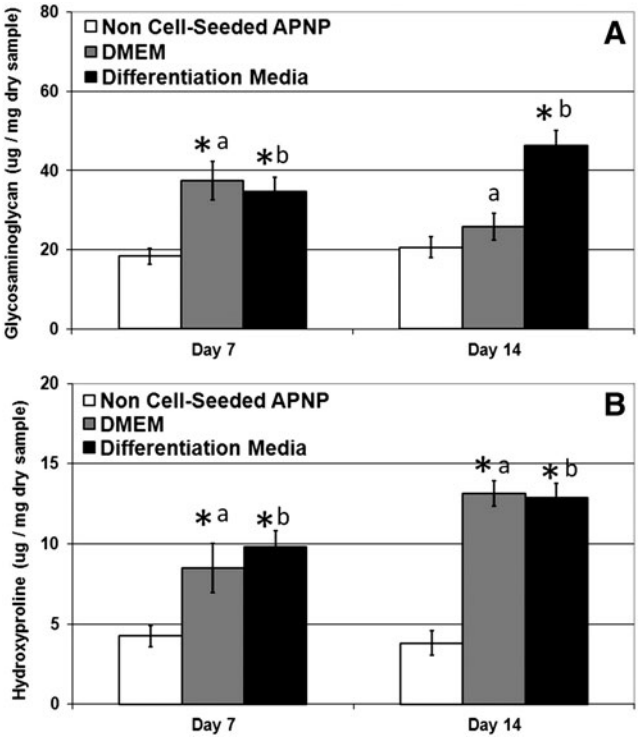

FIG. 2. **(A)** Glycosaminoglycan and **(B)** hydroxyproline content of human-adipose-derived stem cell–seeded APNP hydrogels increased with time in culture as evidenced via comparison to noncell-seeded controls. The symbol * indicates a statistical difference ($p<0.05$) compared with noncell-seeded controls at the corresponding time point. Corresponding letters indicate a significant difference comparing across time points within the respective study group ($n=6$ per study group per time point).

The Hyp content, an indirect measure of total collagen, of hADSC-seeded hydrogels cultured in DMEM for 7 and 14 days (8.49 ± 1.52 and $13.13\pm0.81\,\mu g/mg$ dry weight, respectively) was significantly different ($p<0.05$) compared with nonseeded controls at each respective time point (day 7: 4.25 ± 0.67 and day 14: $3.80\pm0.75\,\mu g/mg$ dry weight) (Fig. 2B). Similarly at day 7 and 14, the Hyp content of hADSC-seeded hydrogels cultured in differentiation media (9.81 ± 1.01 and $12.89\pm0.87\,\mu g/mg$ dry weight) was significantly greater than nonseeded controls at each respective time point ($p<0.05$). When normalized to DNA content, only at the 7-day time point was there a significant difference in Hyp content comparing between hADSC-seeded hydrogels cultured in differentiation media ($64.26\pm6.03\,\mu g/\mu g$ DNA) versus DMEM ($40.39\pm10.18\,\mu g/\mu g$ DNA); by day 14, no difference was observed between study groups. Computed GAG ($\mu g/mg$ dry weight) to Hyp ($\mu g/mg$ dry weight) ratios indicated that hADSC-seeded hydrogels cultured in DMEM exhibited a 2:1 ratio by day 14, whereas those cultured in differentiation media maintained a ratio of ~4:1 throughout the 2-week culture period.

Water content within the hADSC-seeded hydrogels decreased significantly with time in culture ($p<0.05$), regardless of the media type in which they were cultured. Those in DMEM had a water content of $93.58\%\pm0.53\%$ at day 7 that decreased to $91.65\%\pm0.78\%$ by day 14. Likewise, hADSC-seeded hydrogels cultured in differentiation media had a water content of $95.63\%\pm0.44\%$ at day 7 that decreased to $93.05\%\pm0.53\%$ at day 14.

APNP hydrogel contraction measurements

Time course contraction measurements of hADSC-seeded hydrogels were recorded in an attempt to quantify cell-mediated hydrogel remodeling (Fig. 3). Within the first 24 h, hADSC-seeded hydrogels contracted to ~70% of their original surface area and 80% within 48 h. No differences were observed comparing between hydrogels cultured in differentiation media and DMEM during any point in the study. Contraction continued until reaching a steady state at day 9 (Fig. 3), by which time the hydrogels had exhibited a reduction in original surface area of ~90%.

Cell viability and histological analysis

Histological analysis illustrated that the hADSCs were able to infiltrate and disperse throughout the hydrogel material without coercion. LIVE/DEAD fluorescence staining indicated that hADSCs seeded on the hydrogels maintained their viability throughout the 14-day study in both media conditions. Calculations of percent cell viability on APNP hydrogels were not significantly different at day 2 ($90.98\%\pm2.66\%$ viability), day 7 ($88.97\%\pm1.08\%$ viability), or day 14 ($88.39\%\pm2.31\%$ viability) (Fig. 4A). This staining also

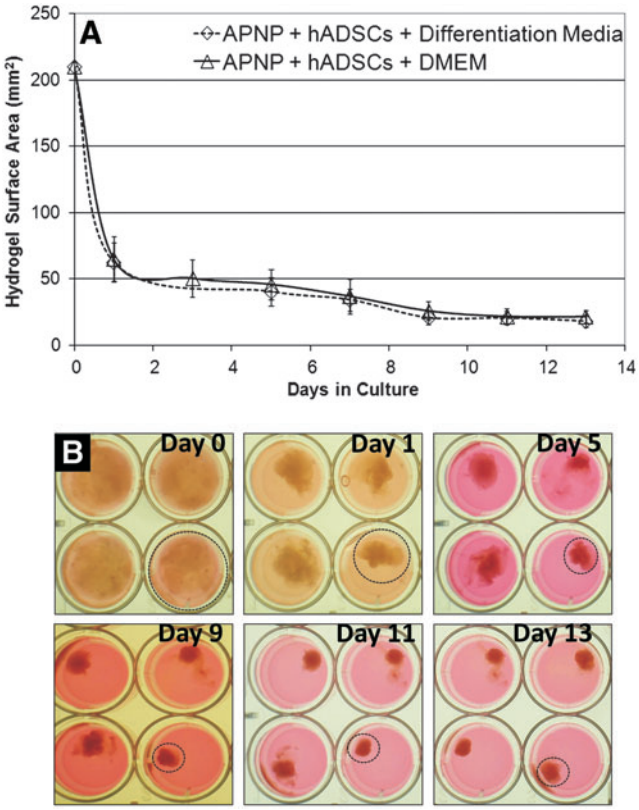

FIG. 3. **(A)** Human-adipose-derived stem cell–seeded APNP hydrogel surface area measurements taken throughout the study and **(B)** corresponding representative time-lapse images tracking four representative cell-seeded hydrogels illustrating cell-mediated contraction (dashed circles highlight the same sample tracked over time in culture) ($n=6$ per study group per time point). Color images available online at www.liebertpub.com/tea

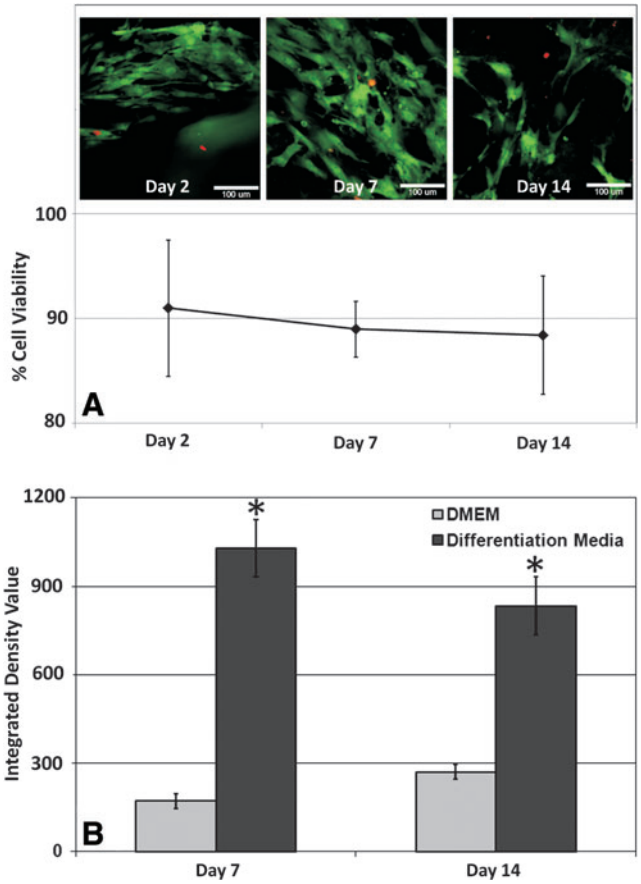

FIG. 4. **(A)** Representative LIVE/DEAD confocal microscopy images of human-adipose-derived stem cells (hADSCs) cultured on APNP hydrogels for 2, 7, and 14 days and quantification indicating no significant difference in cell viability throughout the study period ($n=4$ per study group per time point). **(B)** Matrix metalloproteinase/tissue inhibitors of metalloproteinase (TIMP) array results from hADSCs seeded on APNP hydrogels cultured in DMEM or differentiation media illustrating a significant increase in TIMP-1 levels in the differentiation media group ($n=3$ per study group per time point). Color images available online at www.liebertpub.com/tea

indicated that hADSCs cultured in the APNP hydrogels in DMEM exhibited a mixed morphology, including spindle- and rhombohedral-shaped cells, whereas cells on APNP hydrogels in differentiation media exhibited a predominantly round morphology (Fig. 5A, B). hADSC-seeded hydrogels stained dark with Alcian blue, indicating the presence of GAGs, and pentachrome histology was able to show a qualitative increase in green staining comparing between the differentiation media and DMEM group, indicative of increased GAG content in the differentiation media group (Fig. 6). Conversely, yellow staining appeared more prevalent in the DMEM group as compared with the differentiation media group, indicative of the presence of collagen. Nonseeded controls generally stained diffusely with pentachrome and were difficult to distinguish. Phase-contrast images of hADSCs in monolayer cultured in differentiation media exhibited a polygonal/tetrahedral-shaped morphology (Fig. 5E) while those hADSCs cultured in stromal growth media maintained a characteristic spindle shape (Fig. 5F). Macroscopic images of APNP hydrogels prior to (Fig. 5G) and following cell seeding (Fig. 5H) indicated a transition of opacity with time in culture resulting in a construct that resembled native NP tissue.

MMP/TIMP array analysis

Evaluation of the relative levels of MMPs and TIMPs found within hADSC-seeded APNP hydrogels revealed significantly ($p<0.05$) increased TIMP-1 levels in samples cultured in differentiation media as compared with the DMEM group (Fig. 4B). Neither study group exhibited MMP values above that of nonseeded control samples without hADSCs.

Dynamic mechanical analysis

The response of hADSC-seeded APNP hydrogels to constant cyclic loading and deformation over a range of physiologically relevant frequencies was evaluated following 7 and 14 days of culture. Viscoelastic parameters of complex modulus and phase angle were plotted against test frequency for nonseeded control hydrogels and for hADSC-seeded hydrogels following 7 and 14 days of culture in

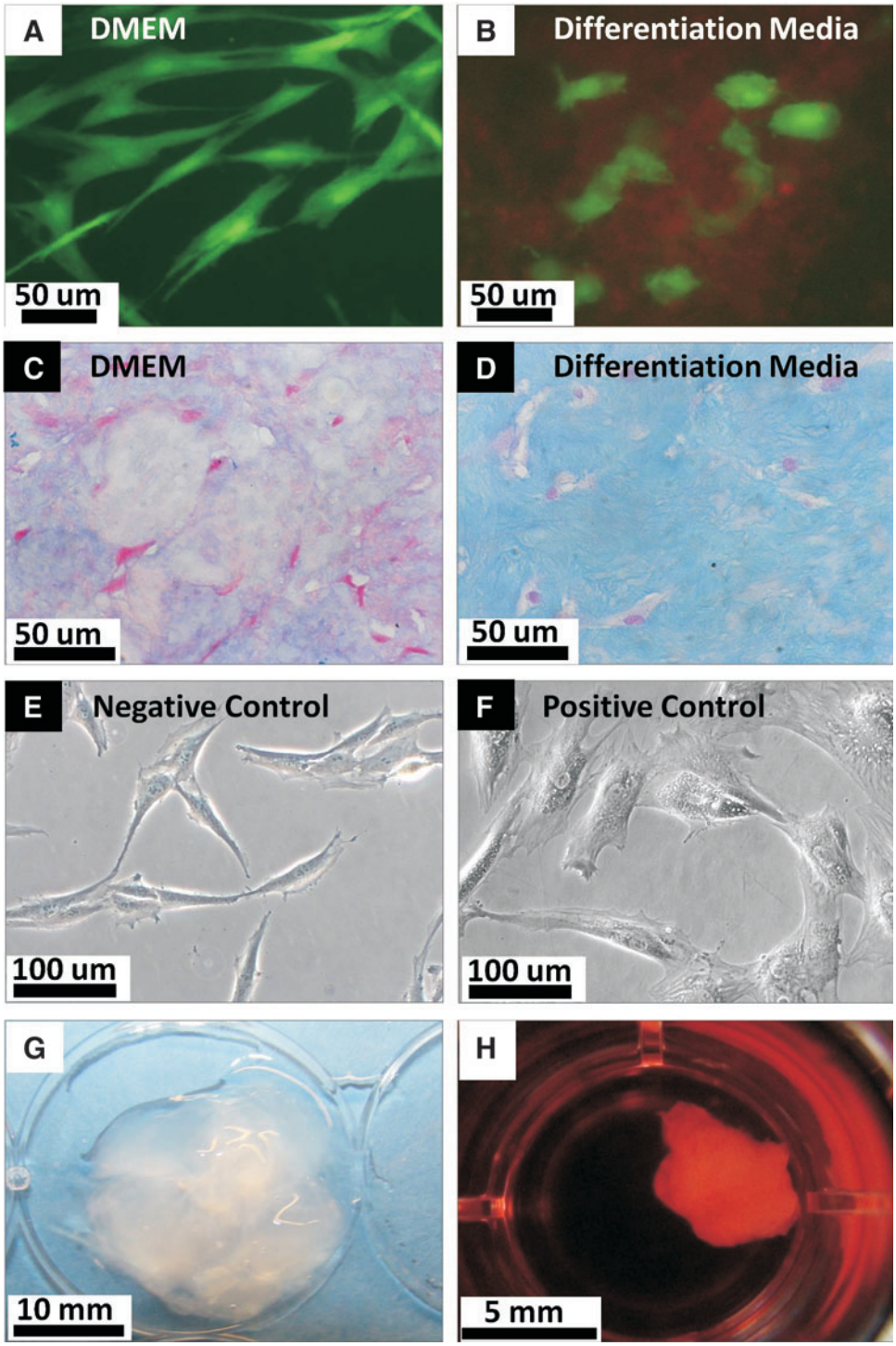

FIG. 5. **(A, B)** Representative LIVE/DEAD (green = live cells; red = dead cells) and **(C, D)** Alcian blue–stained (blue = glycosaminoglycan; red = cell nuclei) hADSC-seeded APNP hydrogels cultured in DMEM or differentiation media, respectively, at 14 days of culture. **(E, F)** Phase-contrast images of hADSCs cultured in monolayer in either DMEM ("negative control") or differentiation media ("positive control"). **(G)** Representative macroscopic images of a noncell-seeded APNP hydrogel and an **(H)** hADSC-seeded hydrogel following 7 days in culture. Color images available online at www.liebertpub.com/tea

differentiation media or DMEM (Fig. 7A, B). Significant differences ($p < 0.05$) were observed comparing the complex modulus values for hADSC-seeded hydrogels following 14 days of culture in differentiation media compared with nonseeded controls for all frequencies tested. Complex modulus values in this group ranged from 16.35 ± 1.42 kPa at 0.1 Hz to 38.36 ± 3.71 kPa at 40 Hz. The complex modulus values for the DMEM group were significantly different from the nonseeded controls at the 10 and 40 Hz frequency following 14 days of culture. Values ranged between 6.95 ± 0.62 kPa at 0.1 Hz and 17.62 ± 1.37 kPa at 40 Hz after 14 days of culture. Nonseeded control values ranged from 5.74 ± 0.40 kPa at 0.1 Hz to 8.74 ± 0.66 kPa at 40 Hz (Fig. 7A). A significant difference in phase angle measurement was observed comparing hADSC-seeded hydrogels following 7 days in culture in differentiation media and DMEM with nonseeded controls for all frequencies tested (Fig. 7B). Following 14 days in culture, the phase angle measurements of the DMEM group remained significantly greater than nonseeded controls for all test frequencies except at 40 Hz;

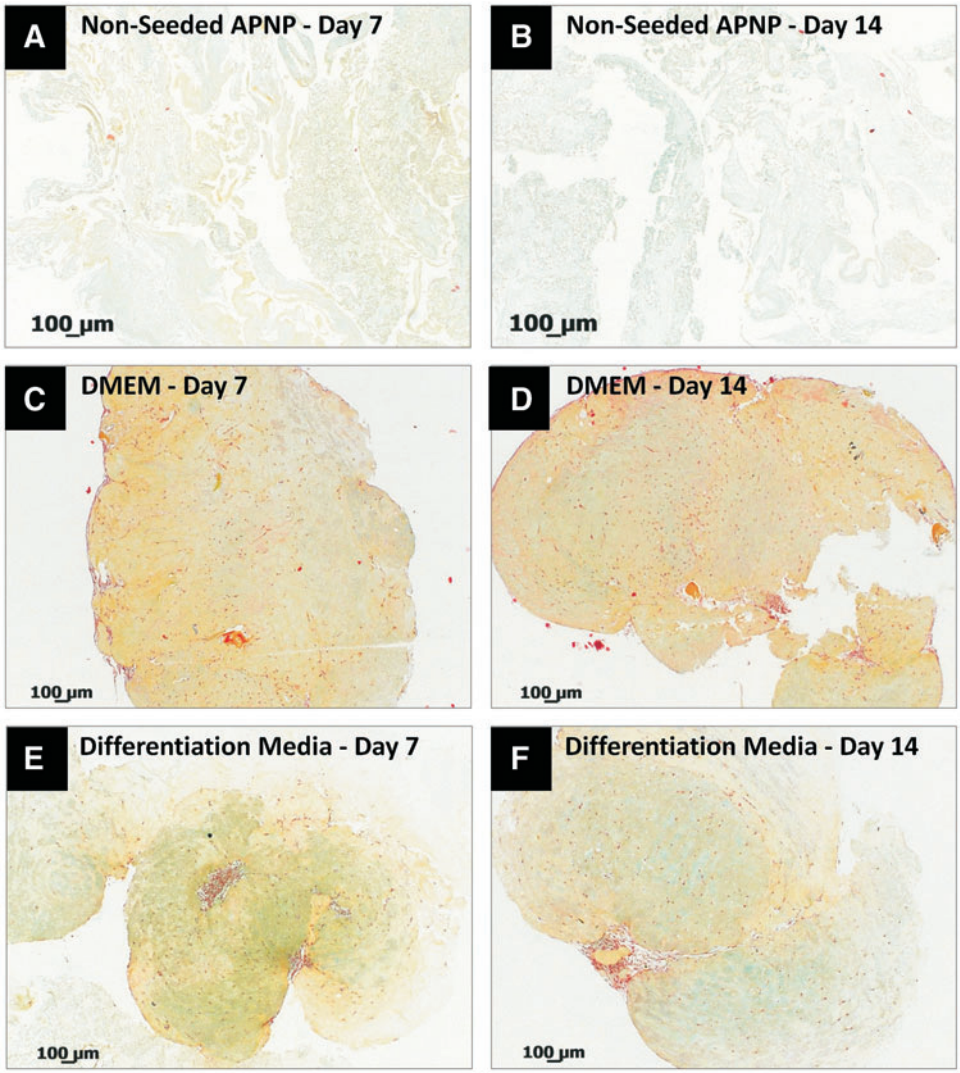

FIG. 6. Representative histological sections of **(A, B)** noncell-seeded APNP hydrogel controls, and hADSC-seeded hydrogels cultured in **(C, D)** DMEM or **(E, F)** differentiation media stained with Movat's Pentachrome after culture for 7 and 14 days indicating increased staining for glycosaminoglycan in the differentiation media group (yellow = collagen, green = glycosaminoglycan, and red = cell nuclei). Color images available online at www.liebertpub.com/tea

however, the differentiation media group was only statistically different at the 10 Hz frequency. Phase angle measurements for hADSC-seeded hydrogels cultured in differentiation media ranged between 10.58 ± 0.48° and 13.10 ± 0.48° following 7 days of culture and 8.73 ± 0.51° and 11.27 ± 0.47° after 14 days of culture over the frequencies tested. Phase angle measurements for hADSC-seeded hydrogels cultured in DMEM ranged between 14.72 ± 1.06° and 17.38 ± 0.77° following 7 days of culture and 8.26 ± 0.73° and 12.41 ± 0.71° after 14 days of culture over the frequencies tested.

In vivo *biocompatibility testing*

All animals survived the initial operation and subsequent 4-week implantation period without any observed complications. Of note, only three out of the eight non-crosslinked APNP hydrogel implants were found at the time of explant. Histological evaluation with Gomori's one-step trichrome staining indicated progressive host cell penetration into all implants (Fig. 8). Average capsule thicknesses surrounding the implants were measured to be 155 ± 25, 194 ± 25, and 224 ± 18 µm for non-crosslinked, EDC/NHS-crosslinked, and EDC/NHS + PGG-crosslinked APNP hydrogels, respectively, which were not found to be statistically different. Immunohistochemistry indicated that infiltrating host cells were predominantly macrophages and fibroblasts with ~5%–10% of the infiltrating cells being $CD8^+$ T-cells (Fig. 9). No remarkable differences in cell type or quantity were noted comparing between the non-crosslinked and crosslinked APNP hydrogels. All hydrogels exhibited evidence of neovascularization, indicated via the presence of multiple blood-filled vessel lumens (Fig. 9), and neo-collagen formation within their interstices as was designated by positive immunohistochemistry for prolyl 4-hydroxylase (Fig. 9). The surrounding adjacent capsule was predominantly composed of fibroblasts, blood vessels, and inflammatory cells; however, some adipose tissue was also observed immediately adjacent to some of the implants. No remarkable differences were observed comparing the host response to any of the APNP hydrogels with that of the HDPE control implants (Fig. 10). No foreign body giant cells or granulomas were noted within any of the samples.

Discussion

Regeneration of tissue relies in large part on the maintenance of a healthy cell phenotype specific for the tissue of

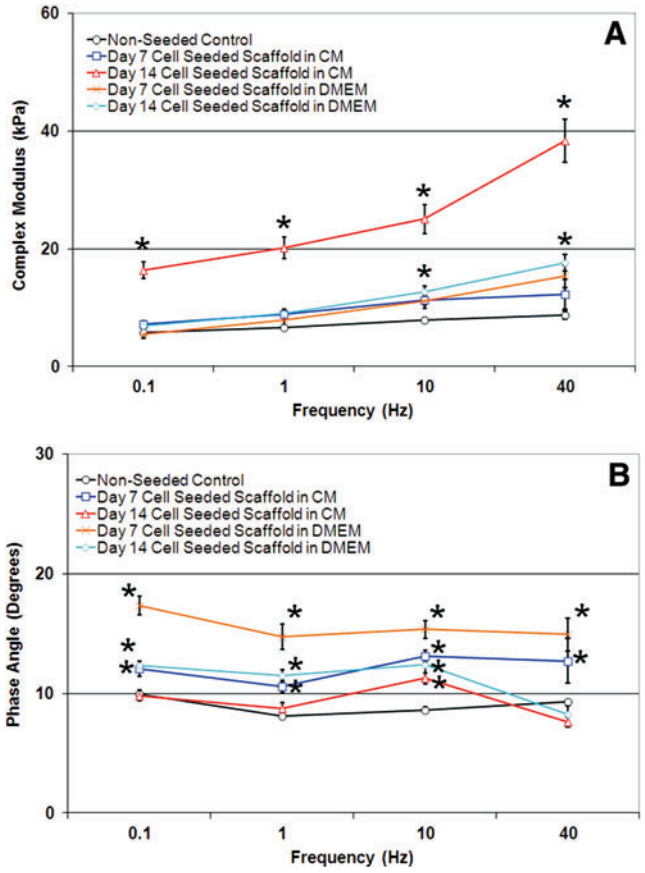

FIG. 7. Graph of **(A)** complex modulus and **(B)** phase angle measurement values for hADSC-seeded APNP hydrogels following 7 and 14 days of culture in differentiation media (CM) or DMEM compared with noncell-seeded hydrogel controls obtained from unconfined compressive dynamic mechanical analysis. The symbol * indicates a statistical difference ($p < 0.05$) compared with noncell-seeded controls at the corresponding test frequency ($n = 5$ per study group per time point). Color images available online at www.liebertpub.com/tea

interest; however, determining discriminating phenotypic markers for the appropriate cell type may prove difficult. This is especially true when attempting to distinguish between a human NP cell and that of an articular chondrocyte. Recent studies by others have begun to shed light on potential distinguishing gene expression profiles for the NP cell.[15–19] In one such attempt, Minogue and colleagues used quantitative PCR analysis to illustrate significantly higher (>50-fold) expression of *PAX-1*, carbonic anhydrase, and Forkhead box 1 in human NP cells compared to articular chondrocytes, thus indicating their putative role as positive NP cell markers.[18] Conversely, the authors noted higher differential expression (>100-fold) of *IBSP* and growth and differentiation factor-10 in articular chondrocytes as compared with NP cells, thus indicating chondrocyte-positive (i.e., NP cell negative) phenotypic markers.[18] Interestingly, the authors were able to illustrate that when cultured in differentiation media on hydrogels, hADSCs appeared to more readily express NP-cell-positive markers and fewer chondrocyte markers as compared with their bone-marrow-derived counterparts, indicating that hADSCs may have more of an affinity toward an NP-cell-like phenotype. Studies performed by Korecki and colleagues have also suggested putative "early NP-cell-" or notochordal-cell-like phenotypic markers, including type III collagen, laminin β-1, and *TIMP-1*.[20] Others have attempted to distinguish between an NP cell and chondrocyte phenotype by comparing their respective tissue ECM gene transcript and protein expression ratios.[21,22]

Herein, we evaluated the ability of our APNP hydrogel to support hADSC differentiation toward an NP cell phenotype by examining traditional NP cell/chondrocyte gene markers as well as using putative human NP cell–positive (*PAX-1*, *TIMP-1*, and type III collagen) and articular chondrocyte-positive (*IBSP*) genes and protein expression markers. Our gene expression results may suggest a mixed phenotype displaying putative gene transcripts representative of both NP cells and chondrocytes. In general, both study groups exhibited evidence of differentiation, likely an effect in part due to the influence of the APNP hydrogel matrix. A recent study by Salzig confirmed that the presence of porcine NP tissue extract combined within a type I collagen hydrogel did elicit differentiation of human mesenchymal stem cells toward a mixed phenotype of NP cells and chondrocytes.[23] Purmessur and colleagues illustrated the ability of porcine NP tissue–conditioned media to influence human stem cell differentiation toward an NP cell phenotype.[24] In their study, stem cells cultured in NP-tissue-conditioned media exhibited significantly increased levels of type II collagen and *TIMP-1* gene transcripts and promoted significantly more GAG production compared with stem cells cultured in basal media and media containing TGF-β_3.[24] The authors go on to suggest that their results indicate differentiation toward an NP cell phenotype as opposed to a chondrocyte that may have been in part due to notochordal-cell-secreted factors. Our gene expression results also appear to fall in line with these findings. It is possible that our APNP hydrogels contain residual porcine-NP- and notochordal-cell-secreted growth factors, and that these factors may steer some of the hADSCs toward an early NP cell or notochordal cell phenotype. Further analysis of the APNP hydrogels needs to be completed to provide a definitive answer to the chemical cues that remain in the APNP hydrogel following decellularization.

We also attempted to directly compare the gene expression profiles of hADSCs on APNP hydrogels to porcine NP and articular cartilage tissues to evaluate the differential expression of NP-positive and -negative gene markers. Direct comparisons were difficult as large differences in the magnitude of the porcine transcript expression compared with hADSCs cultured on APNP hydrogels were observed. The influence of species differences and *in vivo* versus *in vitro* conditions may have contributed to these findings and may be remedied in part by using human NP tissue–derived cells for comparison in future studies. Research by other groups has illustrated that putative NP cell–discriminating markers found in one species may not hold true for others.[17,19,23]

Biochemical data from the present study indirectly indicated that hADSCs were able to produce both GAG and collagen—two extracellular components typically found within the human NP. Healthy human NP typically contains ~450±193 μg GAG/mg sample[25] and exhibits a GAG:Hyp ratio of ~27:1.[22] Higher GAG and Hyp contents were observed in hADSC-seeded hydrogels compared with

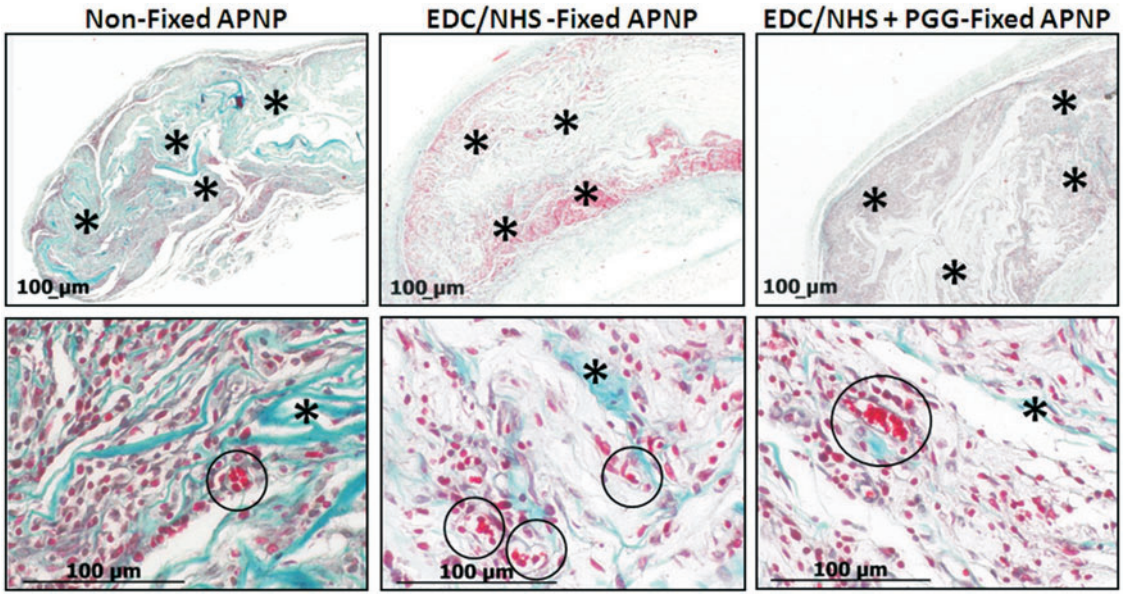

FIG. 8. Representative Gomori's one-step trichrome staining (upper panel) illustrating capsule formation surrounding the implanted APNP hydrogel and (lower panel) hydrogel implant interstices (green = collagen, red = cell nuclei, and circles = blood vessel infiltration containing red blood cells). The symbol * indicates APNP hydrogel material. EDC/NHS, ethyl(dimethylaminopropyl) carbodiimide/N-hydroxysuccinimide. Color images available online at www.liebertpub.com/tea

nonseeded controls for all time points suggested production of these molecules, although confirmation of this should be performed using radioisotope labeling. GAG content and its ratio to Hyp of our hADSC-seeded hydrogels suggest that an NP-tissue-specific ratio was not yet achieved by the study endpoint; however, results by others have indicated that a longer term culture period may be warranted.[26,27] Further, mechanical stimulation has also been shown to greatly affect matrix production and matrix-degrading enzymes in NP cells; therefore, incorporation of physiologically relevant loading conditions in a bioreactor may aid in developing the tissue construct further.[28–31] Culture of stem cells in hypoxic conditions may also help to further differentiate the hADSCs toward an NP cell phenotype on the APNP hydrogels.[32] Of note, the GAG:Hyp ratio of the APNP hydrogel following 2 weeks of culture in differentiation media was higher than the 2:1 ratio reported for human articular cartilage.[22] Cell-mediated remodeling was observed to take place in the APNP hydrogels as evidenced by hydrogel contraction measurements. All hydrogels, regardless of the culture media used, contracted to a similar degree. This phenomenon was the likely result of an attempt by the cells to assemble the hydrogel/matrix into an appropriate tissue. Similar contraction events have been noted in other collagen–GAG-based hydrogels as well.[33–35] It has been shown that human mesenchymal stem cells and chondrocytes express the contractile protein α-smooth muscle actin,[36,37] therefore providing a possible explanation for the phenomenon observed in the present study. Fascinatingly, prior studies by others have illustrated that cell-mediated contraction may help hADSC differentiation toward an NP-cell-like phenotype and may promote NP tissue formation given the appropriate material stiffness of the scaffold.[35] Taken together, the biomimetic nature of the APNP hydrogel, in particular its stiffness, did allow for cell-mediated matrix contraction that along with its biochemical components may have helped to induce hADSC differentiation toward a mixed cell phenotype between that of an NP cell and chondrocyte, even in the absence of differentiation media.

Dynamic mechanical analysis on hADSC-seeded APNP hydrogels indicated an intermittent viscoelastic solid-like behavior, which has been previously reported for human NP tissue.[38,39] In general, complex modulus values illustrated a frequency-dependent behavior. This phenomenon has also been reported by others for the IVD and cartilage.[31,40] Moreover, it was apparent that complex modulus increased with increasing time in culture that was likely the result of cell-mediated contraction, and in the case of the day-14 differentiation media group, this increase could also be attributed to an increase in GAG content. Conversely, phase angle values did not show any frequency dependence but rather a trend toward a reduction in energy dissipation values between 0.1 and 1 Hz with an increased ability to dissipate energy between 10 and 40 Hz. Leahy and Huckins reported a similar minimum in dissipative properties of sheep NP at around 1 Hz.[14] Overall, the dynamic properties of cell-seeded APNP hydrogels approached values calculated in literature for NP tissue.[14,38,41]

Following subdermal implantation of APNP hydrogels, it was observed that the majority of non-crosslinked APNP hydrogels were absent within the subdermal cavity; thus, it was believed that these implants may have degraded completely. Others have observed similar accelerated degradation in non-crosslinked porcine-derived ECM scaffolds.[42] Conversely, Li and colleagues reported that EDC/NHS-crosslinked GAG–collagen scaffolds took at least 3 months to fully degrade.[43] In the present study, it was clear from histological and immunohistochemical characterization of the remaining APNP hydrogels that an inflammatory response was ongoing at 4 weeks. This was likely the result of delayed

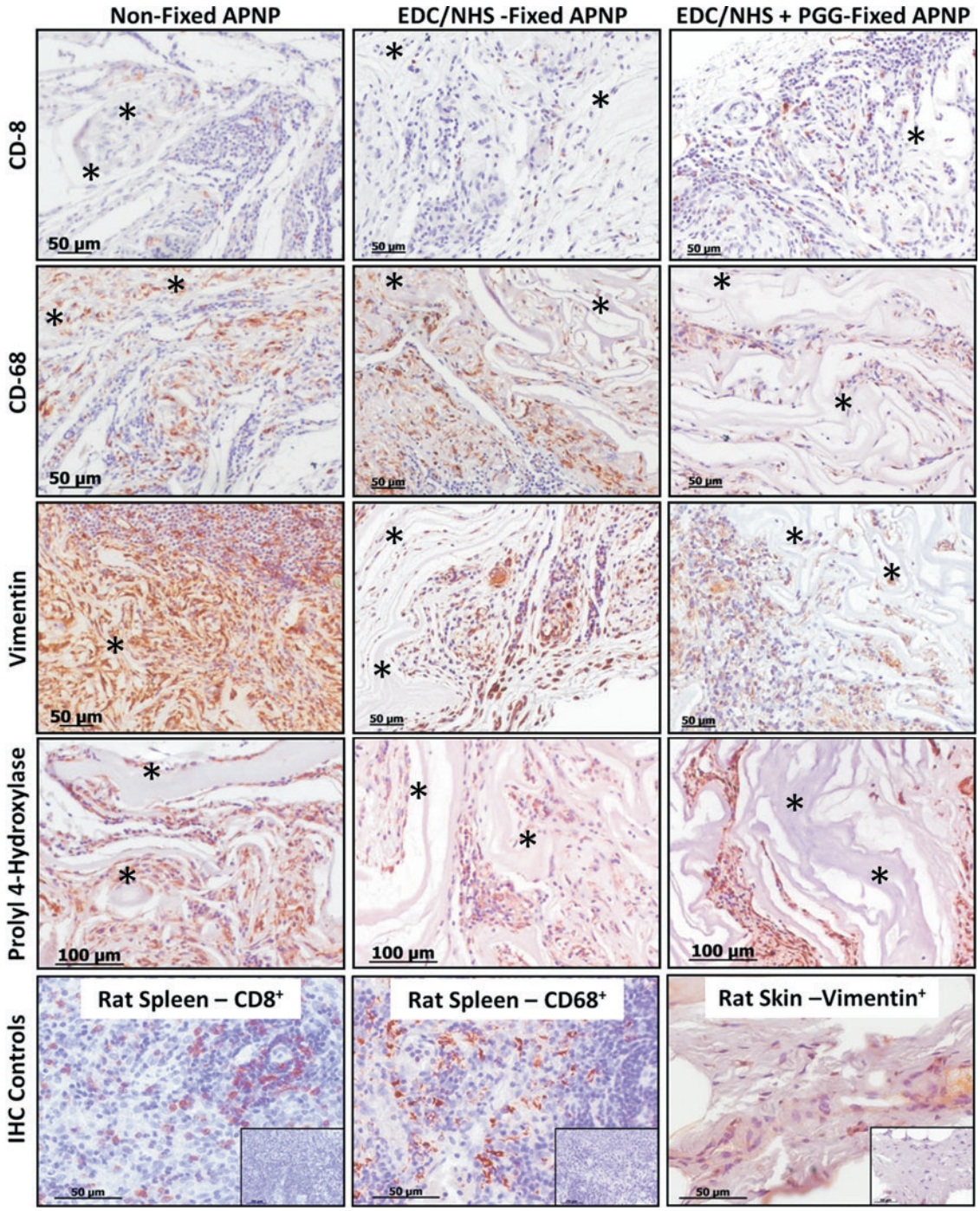

FIG. 9. Representative histological sections of chemically crosslinked ("fixed") and non-crosslinked ("nonfixed") APNP hydrogels explanted after 1 month of subdermal implantation in rats. Immunohistochemical staining performed to detect cytotoxic T-cells (CD-8), macrophages (CD-68), fibroblasts (vimentin), and neo-collagen production (prolyl 4-hydroxylase) (brown = positive staining; blue = cell nuclei) within the hydrogel interstices. Rat spleen: positive IHC control for T-cells and macrophages, and rat skin for fibroblasts (insets = negative controls). The symbol * indicates APNP hydrogel material. Color images available online at www.liebertpub.com/tea

degradation and persistent presence of the xenogenic material due to crosslinking.[44] Additionally, the potential intrinsic interaction of the GAG present in APNP hydrogels with proinflammatory cytokines may play a role in developing the observed response.[45] Moreover, some suggest that autologous NP tissue is proinflammatory and can elicit an autoimmune reaction once outside the confines of the annulus fibrosus.[46–48] Overall, however, APNP hydrogels appeared to exhibit evidence of neovascularization, mononuclear cellular infiltration, and deposition of host-derived ECM indicative of progressive tissue remodeling.[42,49]

It is evident from the studies contained herein that the APNP hydrogels support progressive differentiation of hADSCs away from an undifferentiated stem cell state.

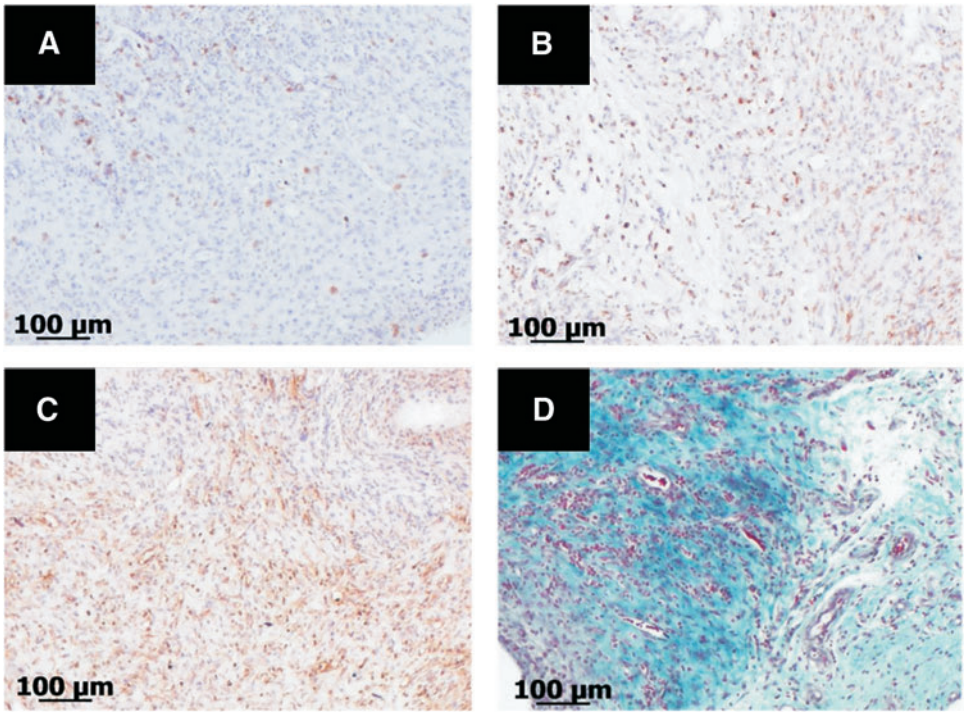

FIG. 10. Representative histological sections of host tissue surrounding high-density polyethylene negative control implants stained immunohistochemically for **(A)** cytotoxic T-cells, **(B)** macrophages, **(C)** fibroblasts (brown = positive staining; blue = cell nuclei), and with **(D)** Gomori's one-step trichrome (green = collagen; red = cell nuclei). Color images available online at www.liebertpub.com/tea

Whether or not the resultant cell phenotype is purely that of an NP cell, a chondrocyte, or a combination of both cell types remains to be determined. Regardless however, the cells are differentiating on the APNP hydrogels and this differentiation process may aid in protecting these cells when implanted into the harsh environment of the IVD. Studies have indicated that undifferentiated stem cells do not fare well when placed into an environment reminiscent of the IVD.[50–52] It appears that the low pH and high osmolarity of the IVD decrease viability, proliferation, and matrix production of mesenchymal stem cells.[50–52] Thus, "predifferentiation" of stem cells toward a phenotype that may be better adapted to such an environment may be beneficial. Given the evidence contained herein, it appears that the APNP hydrogel does support differentiation of stem cells toward a phenotype that may be adapted for the IVD environment. This has translational implications in that porcine NP is readily available in large quantities for decellularization and thus an off-the-shelf material would be available for patient use in conjunction with autologous stem cells. Additionally, if differentiation can be achieved on a scaffold without the use of exogenous growth factors, the commercial approval pathway of such a material may be less daunting.

Conclusions

Results of this study illustrate that APNP hydrogels may serve as an effective scaffold for NP tissue engineering. The hydrogels do support human stem cell differentiation toward an appropriate phenotype and allow for cellular remodeling while exhibiting evidence of an acceptable *in vivo* host response following implantation.

Disclosure Statement

No competing financial interests exist.

References

1. An, H.S., Thonar, E.J., and Masuda, K. Biological repair of intervertebral disc. Spine **28,** S86, 2003.
2. Quality AfHR. Healthcare Cost & Utilization Project. 2009.
3. Haefeli, M., Kalberer, F., Saegesser, D., Nerlich, A.G., Boos, N., and Paesold, G. The course of macroscopic degeneration in the human lumbar intervertebral disc. Spine **31,** 1522, 2006.
4. Boos, N., Weissbach, S., Rohrbach, H., Weiler, C., Spratt, K.F., and Nerlich, AG. Classification of age-related changes in lumbar intervertebral discs: 2002 Volvo Award in basic science. Spine (Phila Pa 1976) **27,** 2631, 2002.
5. Adams, M.R.P. What is intervertebral disc degeneration, and what causes it? Spine **31,** 2151, 2006.
6. Roughley, P.J. Biology of intervertebral disc aging and degeneration: involvement of the extracellular matrix. Spine **29,** 2691, 2004.
7. Calderon, L., Collin, E., Velasco-Bayon, D., Murphy, M., O'Halloran, D., and Pandit, A. Type II collagen-hyaluronan hydrogel—a step towards a scaffold for intervertebral disc tissue engineering. Eur Cell Mater **20,** 134, 2010.
8. Chou, A.I., Akintoye, S.O., and Nicoll, S.B. Photo-crosslinked alginate hydrogels support enhanced matrix accumulation by nucleus pulposus cells *in vivo*. Osteoarthritis Cartilage **17,** 1377, 2009.
9. Collin, E.C., Grad, S., Zeugolis, D.I., Vinatier, C.S., Clouet, J.R., Guicheux, J.J., Weiss, P., Alini, M., and Pandit, A.S. An injectable vehicle for nucleus pulposus cell-based therapy. Biomaterials **32,** 2862, 2011.
10. Yang, S.H., Chen, P.Q., Chen, Y.F., and Lin, F.H. An *in-vitro* study on regeneration of human nucleus pulposus by using gelatin/chondroitin-6-sulfate/hyaluronan tri-copolymer scaffold. Artif Organs **29,** 806, 2005.
11. Mercuri, J.J., Gill, S.S., and Simionescu, D.T. Novel tissue-derived biomimetic scaffold for regenerating the human nucleus pulposus. J Biomed Mater Res A **96,** 422, 2010.

12. Farndale, R.W., Buttle, D.J., and Barrett, A.J. Improved quantitation and discrimination of sulphated glycosaminoglycans by use of dimethylmethylene blue. Biochim Biophys Acta **883,** 173, 1986.
13. Blumenkrantz, N., and Asboe-Hansen, G. An assay for hydroxyproline and proline on one sample and a simplified method for hydroxyproline. Anal Biochem **63,** 331, 1975.
14. Leahy, J.C., and Hukins, D.W. Viscoelastic properties of the nucleus pulposus of the intervertebral disk in compression. J Mater Sci Mater Med **12,** 689, 2001.
15. Chen, J., Jing, L., Gilchrist, C.L., Richardson, W.J., Fitch, R.D., and Setton, L.A. Expression of laminin isoforms, receptors, and binding proteins unique to nucleus pulposus cells of immature intervertebral disc. Connect Tissue Res **50,** 294, 2009.
16. Gilchrist, C.L., Chen, J., Richardson, W.J., Loeser, R.F., and Setton, L.A. Functional integrin subunits regulating cell-matrix interactions in the intervertebral disc. J Orthop Res **25,** 829, 2007.
17. Lee, C.R., Sakai, D., Nakai, T., Toyama, K., Mochida, J., Alini, M., and Grad, S. A phenotypic comparison of intervertebral disc and articular cartilage cells in the rat. Eur Spine J **16,** 2174, 2007.
18. Minogue, B.M., Richardson, S.M., Zeef, L.A., Freemont, A.J., and Hoyland, J.A. Characterization of the human nucleus pulposus cell phenotype and evaluation of novel marker gene expression to define adult stem cell differentiation. Arthritis Rheum **62,** 3695, 2011.
19. Sakai, D., Nakai, T., Mochida, J., Alini, M., and Grad, S. Differential phenotype of intervertebral disc cells: microarray and immunohistochemical analysis of canine nucleus pulposus and annulus fibrosus. Spine (Phila Pa 1976) **34,** 1448, 2009.
20. Korecki, C.L., Taboas, J.M., Tuan, R.S., and Iatridis, J.C. Notochordal cell conditioned medium stimulates mesenchymal stem cell differentiation toward a young nucleus pulposus phenotype. Stem Cell Res Ther **1,** 18, 2010.
21. Clouet, J., Grimandi, G., Pot-Vaucel, M., Masson, M., Fellah, H.B., Guigand, L., Cherel, Y., Bord, E., Rannou, F., Weiss, P., and others. Identification of phenotypic discriminating markers for intervertebral disc cells and articular chondrocytes. Rheumatology (Oxford) **48,** 1447, 2009.
22. Mwale, F., Roughley, P., and Antoniou, J. Distinction between the extracellular matrix of the nucleus pulposus and hyaline cartilage: a requisite for tissue engineering of intervertebral disc. Eur Cell Mater **8,** 58, 2004.
23. Salzig, D., Schmiermund, A., Gebauer, E., Fuchsbauer, H., and Czermak, P. Influence of porcine intervertebral disc matrix on stem cell differentiation. J Funct Biomater **2,** 155, 2011.
24. Purmessur, D., Schek, R.M., Abbott, R.D., Ballif, B.A., Godburn, K.E., and Iatridis, J.C. Notochordal conditioned media from tissue increases proteoglycan accumulation and promotes a healthy nucleus pulposus phenotype in human mesenchymal stem cells. Arthritis Res Ther **13,** R81, 2011.
25. Nguyen, A.M., Johannessen, W., Yoder, J.H., Wheaton, A.J., Vresilovic, E.J., Borthakur, A., and Elliott, D.M. Noninvasive quantification of human nucleus pulposus pressure with use of T1rho-weighted magnetic resonance imaging. J Bone Joint Surg Am **90,** 796, 2008.
26. Alini, M., Li, W., Markovic, P., Aebi, M., Spiro, R.C., and Roughley, P.J. The potential and limitations of a cell-seeded collagen/hyaluronan scaffold to engineer an intervertebral disc-like matrix. Spine **28,** 446, 2003; discussion 453.
27. Seguin, C.A., Grynpas, M.D., Pilliar, R.M., Waldman, S.D., and Kandel, R.A. Tissue engineered nucleus pulposus tissue formed on a porous calcium polyphosphate substrate. Spine (Phila Pa 1976) **29,** 1299, 2004.
28. Handa, T., Ishihara, H., Ohshima, H., Osada, R., Tsuji, H., and Obata, K. Effects of hydrostatic pressure on matrix synthesis and matrix metalloproteinase production in the human lumbar intervertebral disc. Spine **22,** 1085, 1997.
29. Maclean, J.J., Lee, C.R., Alini, M., and Iatridis, J.C. Anabolic and catabolic mRNA levels of the intervertebral disc vary with the magnitude and frequency of *in vivo* dynamic compression. J Orthop Res **22,** 1193, 2004.
30. Wang, D.L., Jiang, S.D., and Dai, L.Y. Biologic response of the intervertebral disc to static and dynamic compression *in vitro*. Spine (Phila Pa 1976) **32,** 2521, 2007.
31. Walsh, A.J., and Lotz, J.C. Biological response of the intervertebral disc to dynamic loading. J Biomech **37,** 329, 2004.
32. Risbud, M.V., Albert, T.J., Guttapalli, A., Vresilovic, E.J., Hillibrand, A.S., Vaccaro, A.R., and Shapiro, I.M. Differentiation of mesenchymal stem cells towards a nucleus pulposus-like phenotype *in vitro*: implications for cell-based transplantation therapy. Spine (Phila Pa 1976) **29,** 2627, 2004.
33. Halloran, D.O., Grad, S., Stoddart, M., Dockery, P., Alini, M., and Pandit, A.S. An injectable cross-linked scaffold for nucleus pulposus regeneration. Biomaterials **29,** 438, 2008.
34. Tang, S., and Spector, M. Incorporation of hyaluronic acid into collagen scaffolds for the control of chondrocyte-mediated contraction and chondrogenesis. Biomed Mater **2,** S135, 2007.
35. Vickers, S.M., Squitieri, L.S., and Spector, M. Effects of cross-linking type II collagen-GAG scaffolds on chondrogenesis *in vitro*: dynamic pore reduction promotes cartilage formation. Tissue Eng **12,** 1345, 2006.
36. Kinner, B., and Spector, M. Smooth muscle actin expression by human articular chondrocytes and their contraction of a collagen-glycosaminoglycan matrix *in vitro*. J Orthop Res **19,** 233, 2001.
37. Kinner, B., Zaleskas, J.M., and Spector, M. Regulation of smooth muscle actin expression and contraction in adult human mesenchymal stem cells. Exp Cell Res **278,** 72, 2002.
38. Iatridis, J.C., Weidenbaum, M., Setton, L.A., and Mow, V.C. Is the nucleus pulposus a solid or a fluid? Mechanical behaviors of the nucleus pulposus of the human intervertebral disc. Spine **21,** 1174, 1996.
39. Johannessen, W., and Elliott, D.M. Effects of degeneration on the biphasic material properties of human nucleus pulposus in confined compression. Spine **30,** E724, 2005.
40. Fulcher, G.R., Hukins, D.W., and Shepherd, D.E. Viscoelastic properties of bovine articular cartilage attached to subchondral bone at high frequencies. BMC Musculoskelet Disord **10,** 61, 2009.
41. Iatridis, J.C., Setton, L.A., Weidenbaum, M., and Mow, V.C. The viscoelastic behavior of the non-degenerate human lumbar nucleus pulposus in shear. J Biomech **30,** 1005, 1997.
42. Badylak, S.F. Xenogeneic extracellular matrix as a scaffold for tissue reconstruction. Transpl Immunol **12,** 367, 2004.
43. Li, C.Q., Huang, B., Luo, G., Zhang, C.Z., Zhuang, Y., and Zhou, Y. Construction of collagen II/hyaluronate/chondroitin-6-sulfate tri-copolymer scaffold for nucleus pulposus tissue engineering and preliminary analysis of its physico-chemical properties and biocompatibility. J Mater Sci Mater Med **21,** 741, 2009.

44. Badylak, S.F., and Gilbert, T.W. Immune response to biologic scaffold materials. Semin Immunol **20,** 109, 2008.
45. Ramsden, L., and Rider, C.C. Selective and differential binding of interleukin (IL)-1 alpha, IL-1 beta, IL-2 and IL-6 to glycosaminoglycans. Eur J Immunol **22,** 3027, 1992.
46. Geiss, A., Larsson, K., Junevik, K., Rydevik, B., and Olmarker, K. Autologous nucleus pulposus primes T cells to develop into interleukin-4-producing effector cells: an experimental study on the autoimmune properties of nucleus pulposus. J Orthop Res **27,** 97, 2009.
47. Geiss, A., Larsson, K., Rydevik, B., Takahashi, I., and Olmarker, K. Autoimmune properties of nucleus pulposus: an experimental study in pigs. Spine (Phila Pa 1976) **32,** 168, 2007.
48. Murai, K., Sakai, D., Nakamura, Y., Nakai, T., Igarashi, T., Seo, N., Murakami, T., Kobayashi, E., and Mochida, J. Primary immune system responders to nucleus pulposus cells: evidence for immune response in disc herniation. Eur Cell Mater **19,** 13, 2010.
49. Anderson, J.M., Rodriguez, A., and Chang, D.T. Foreign body reaction to biomaterials. Semin Immunol **20,** 86, 2008.
50. Liang, C., Li, H., Tao, Y., Zhou, X., Li, F., Chen, G., and Chen, Q. Responses of human adipose-derived mesenchymal stem cells to chemical microenvironment of the intervertebral disc. J Transl Med **10,** 49, 2012.
51. Wuertz, K., Godburn, K., and Iatridis, J.C. MSC response to pH levels found in degenerating intervertebral discs. Biochem Biophys Res Commun **379,** 824, 2009.
52. Wuertz, K., Godburn, K., Neidlinger-Wilke, C., Urban, J., and Iatridis, J.C. Behavior of mesenchymal stem cells in the chemical microenvironment of the intervertebral disc. Spine (Phila Pa 1976) **33,** 1843, 2008.

Address correspondence to:
Dan T. Simionescu, PhD
Department of Bioengineering
Clemson University
304 Rhodes Engineering Research Center—Annex
Clemson, SC 29634

E-mail: dsimion@clemson.edu

Received: February 11, 2012
Accepted: November 08, 2012
Online Publication Date: January 7, 2013